High resolution, large field of view x-ray differential phase contrast imaging on a compact setup

Thuering, T ; Modregger, P ; Grund, T ; Kenntner, J ; David, C ; Stampanoni, M

DOI: https://doi.org/10.1063/1.3618672

AIP | Applied Physics Letters

High resolution, large field of view x-ray differential phase contrast imaging on a compact setup

T. Thuering, P. Modregger, T. Grund, J. Kenntner, C. David et al.

Citation: Appl. Phys. Lett. **99**, 041111 (2011); doi: 10.1063/1.3618672
View online: http://dx.doi.org/10.1063/1.3618672
View Table of Contents: http://apl.aip.org/resource/1/APPLAB/v99/i4
Published by the American Institute of Physics.

High resolution, large field of view x-ray differential phase contrast imaging on a compact setup

T. Thuering,[1,2,a)] P. Modregger,[1,3] T. Grund,[4] J. Kenntner,[4] C. David,[5] and M. Stampanoni[1,2]
[1]*Swiss Light Source, Paul Scherrer Institut, Villigen PSI, Switzerland*
[2]*Institute for Biomedical Engineering, Swiss Federal Institute of Technology, Zurich, Switzerland*
[3]*School of Biology and Medicine, University of Lausanne, Lausanne, Switzerland*
[4]*Karlsruhe Nano Micro Facility (KNMF), Karlsruhe Institute of Technology (KIT), Karlsruhe, Germany*
[5]*Laboratory for Micro- and Nanotechnology, Paul Scherrer Institut, Villigen PSI, Switzerland*

(Received 1 June 2011; accepted 10 July 2011; published online 28 July 2011)

X-ray grating interferometry is a well established technique to perform differential phase contrast imaging on conventional x-ray tubes. So far, the application of this technique in commercial micro computed tomography scanners has remained a major challenge due to the compact setup geometry. In this letter, we report on the design of a compact imaging setup using a microfocus source. Due to the extreme wave front curvature, the gratings are fabricated on a flexible substrate, enabling precise cylindrical shaping. A laboratory setup and a modified SCANCO μCT100 scanner have been built, allowing high resolution and large field of view imaging. © *2011 American Institute of Physics*. [doi:10.1063/1.3618672]

Grating interferometry provides a multi-modal x-ray imaging technique. Conventional absorption as well as phase[1–3] and dark field[4] contrast signals are acquired in parallel and can yield perceptually and quantitatively complementary information about an examined object. The three signals are related to the attenuation, the phase shift and the scattering, respectively, of radiation, induced by the sample. Due to the ability of measuring the differential phase signal, the technique is also often referred to as differential phase contrast (DPC) imaging. Depending on the sample and the x-ray energy, the contrast in phase or dark field images can be superior to absorption images. For instance in the hard x-ray regime, phase sensitive images can provide considerably higher contrast than standard absorption-based images for biological tissue.[5]

The most prominent advantage of grating interferometry is the applicability on conventional x-ray tubes. A source grating can be used to generate an array of individually coherent, but mutually incoherent x-ray sources.[6] An alternative approach is the use of microfocus tubes, generally providing enough spatial beam coherence for the interference formation.[7]

Recently proposed setups[6,7] either provide high resolution or large field of view (FOV) imaging. Here, we present a DPC imaging setup, which simultaneously allows both, high geometric magnification and a large FOV. In addition, the system is compact enough for the integration into a commercial micro computed tomography (CT) device, and thus, the setup has also been implemented on a SCANCO μCT 100 scanner.

Fig. 1 shows a DPC setup based on a microfocus source. A phase grating with a line period of a few microns introduces a periodic phase shift of π in the wave front and generates an interference pattern downstream. Under coherent illumination, maximal interference occurs at fractional Talbot distances away from the phase grating, given by $d_m = mp_1^2/8\lambda$, where m is the fractional Talbot order, p_1 is the pitch of the phase grating, and λ is the wavelength. At this position, an absorption grating with a pitch matching the period of the interference fringes is placed. Attenuation, refraction, and scattering of the beam, induced by an object, alter the interference pattern, each in a distinct way. Attenuation leads to an intensity reduction, refraction laterally shifts the fringes, and scattering reduces fringe visibility.

A typical acquisition protocol for imaging is based on a "phase stepping" scan. Either of the two gratings is moved in equidistant steps over a grating period along the transverse beam direction and images are acquired at every step position.[3] The result is an intensity oscillation (phase stepping curve) recorded in each pixel. In an imaging experiment, both a reference and an object phase stepping scan are acquired. Image formation is then performed by the quantification of the above effects through the analysis of the reference and object scans. An important parameter in terms of the contrast-to-noise ratio in differential phase and dark-field images is the signal visibility, $V = a_1^r/a_0^r$, where a_i^r is the absolute value of the ith Fourier coefficient of the reference phase stepping curve.

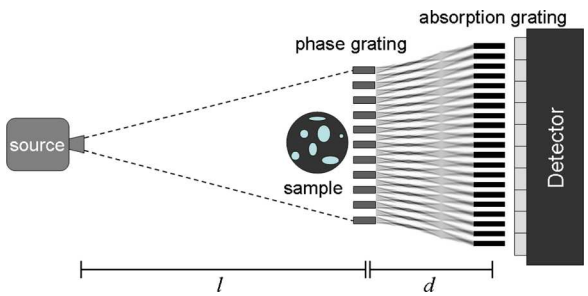

FIG. 1. (Color online) Schematic of a DPC imaging setup using a grating interferometer. The interference pattern is generated by the phase grating. The absorption grating is used to analyze the interference fringes.

a)Author to whom correspondence should be addressed. Electronic mail: thomas.thuering@psi.ch.

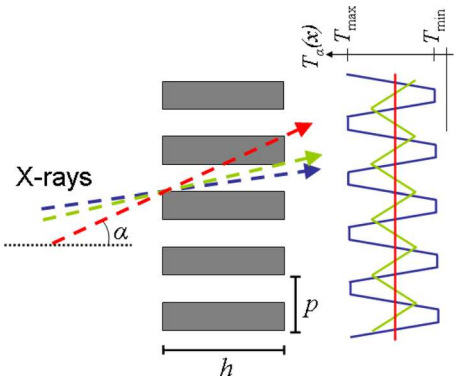

FIG. 2. (Color online) X-rays with an incident angle, α, close to $2/AR = p/h$ encounter an altered transmission function $T_\alpha(x)$ of the grating.

Advancing towards the development of a compact setup for the application of DPC imaging in industrial micro CT scanners has remained a challenging task. Today's micro CT systems encompass stand-alone solutions with a compact table-top design. High resolution is achieved by using microfocus x-ray sources, which provide a reasonable photon flux for a compact source-to-detector distance. The cone beam geometry, enabling high magnification and a large FOV, is a typical feature of such systems. However, the short source-to-grating distance implies a high wave front curvature, causing major limitations for grating interferometry using planar grating substrates.[8] The typically high aspect ratio $AR = 2h/p$ of the grating structures, where p is the period and h the structure height, leads to a significant change of the grating transmission function for x-rays impinging at angles close to $\arctan(2/AR)$ (Fig. 2). For $\tan(\alpha) = 2/AR \approx \alpha$, the transmission function of the phase grating becomes flat, preventing the interference pattern formation. Similarly, the altered transmission function of the absorption grating results in a reduced efficiency for the fringe detection. Ultimately, this degradation leads, in both cases, to a loss in signal visibility. This issue becomes particularly problematic at higher photon energies, where the structure height of the absorption grating needs to be large in order to maintain high absorption amplitudes in the transmission function.

The loss of signal visibility at large incident angles reduces the FOV. Assuming that $\alpha = 2/AR$ represents the upper limit for the divergence angle, the maximum available FOV for an imaging setup with a source-to-sample distance of l_s is given by

$$\mathrm{FOV}_{\max,\mathrm{pg}} = \frac{4l_s}{AR_{\max}}. \quad (1)$$

$AR_{\max}$ is related to the critical component, which is, in general, the absorption grating. For instance, a source-to-sample distance of $l_s = 250$ mm (typcial for a compact micro CT) and an aspect ratio of $AR_{g2} = 50$ would limit the FOV to 20 mm. In practice, the visibility already decays significantly before $\alpha = 2/AR$ and, therefore, the FOV is expected to be even smaller than the value given in Eq. (1).

Fig. 3(a) demonstrates the signal loss at large angles in a differential phase radiography of a plastic screw and Fig. 3(c) shows the associated visibility profile using planar gratings. The scans were acquired at an x-ray tube setup with a total

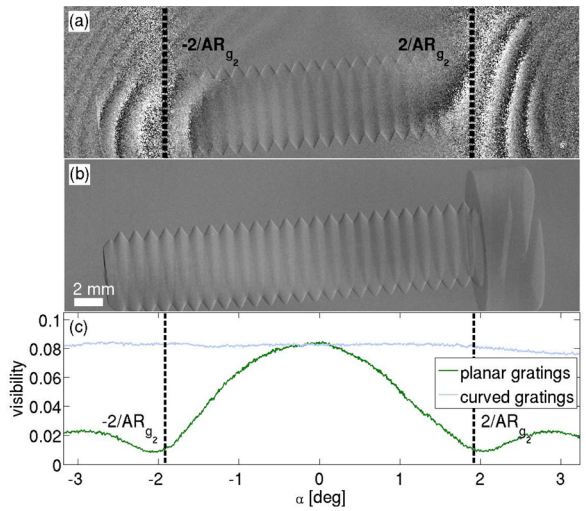

FIG. 3. (Color online) Differential phase contrast images obtained from a scan with (a) planar gratings and (b) curved gratings. (c) shows the visibility profile for both cases.

length of $s = 340$ mm. The phase grating was designed for a photon energy of 28 keV, and the pitches of the phase and the absorption gratings were $p_1 = 4.12$ μm and $p_2 = 2.4$ μm, respectively. Given these settings, the fractional Talbot order of the inter-grating distance amounts to $m = 0.83$. The acceleration voltage of the tube was 50 kV and the anode current 85 μA. A phase stepping scan with 16 steps and an exposure time of 5 s for each step has been acquired over two periods of the absorption grating. The effective pixel size of the image is $p_{\mathrm{eff}} = 36$ μm. The aspect ratios of the gratings were $AR_{g1} \approx 4.8$ and $AR_{g2} \approx 48$, respectively. Evidently, the absorption grating is the critical component which dramatically limits the FOV. The unit on the horizontal detector axis in Fig. 3 was converted to the incident angle α and the positions where $\alpha = \pm 2/AR$ are marked with a dashed line. At this position, the visibility decays to a minimum and thus, no differential phase signal was measured.

The degradation of the grating transmission function for high incident angles can be avoided by matching the grating shape to the wave front curvature. This requires the fabrication of cylindrically-shaped gratings with a bending radius corresponding to the source-to-grating distance. Revol *et al.* already proposed the usage of bent gratings;[9] however, the bending radius was restricted ($r > 50$ cm), most likely due to the substrate material. The setup length in compact micro CT systems usually implies bending radii, which cannot be achieved by currently-used substrates (e.g., silicon wafers). We found titanium, a suitable substrate material for the fabrication of curved gratings. With substrate thicknesses between 50 and 140 μm, the titanium foils are highly flexible for deformation, cause only low absorption losses (approximately 10% at 30 keV for 50 μm Ti) and allow precise cylindrical shaping. Moreover, it is compatible with x-ray lithography and electroplating fabrication processes,[10] using nickel as phase shifting material and gold for the absorbing structures. The dimensions of the gratings are 20 mm along the grating lines and 60 mm in the perpendicular direction.

Using cylindrically-shaped gratings, the limitation of the FOV is no longer dependent on the beam divergence angle

and the aspect ratio of the gratings, but solely on the grating and detector dimensions and on the setup length. In case the size of the gratings is the limiting factor, the maximum FOV is given by

$$\mathrm{FOV}_{\mathrm{max,cg}} = 2l_s \tan\left(\frac{b_{g_2}}{2s}\right) \approx l_s \frac{b_{g_2}}{s}, \tag{2}$$

where b_{g2} is the arc length of the absorption grating in perpendicular line direction. Using the previous parameters ($l_s = 250$ mm and $s = 340$ mm) and with $b_{g2} = 60$ mm, the maximum FOV becomes $\mathrm{FOV}_{\mathrm{max,cg}} \approx 44$ mm. Compared to the FOV with planar gratings, this is more than a two-fold increase.

Fig. 3(b) shows the differential phase image of the plastic screw and Fig. 3(c) displays the visibility profile using curved gratings. Setup and grating parameters were the same as for the experiment with planar gratings. The homogeneous visibility profile over the full detector plane and the strong image contrast at large incident angles demonstrate the significant increase in FOV. In principle, phase stepping would need to be performed on the circular trajectory given by the shape of the absorption grating. Due to the negligible error in travelling distance, conventional linear phase stepping was performed.

The combination of a small focal spot, obtained by a microfocus source, and the curved shape of the gratings allows high resolution and large FOV imaging at the same time. High resolution is achieved by means of geometric magnification. The geometric magnification factor $M = s/l_s$ is chosen through the source-to-sample distance l_s. However, the increase in resolution is limited by the geometric unsharpness, which is dependent on the finite source width. When the unsharpness exceeds the pixel size, a further increase of the magnification factor no longer improves resolution.[11] It can be shown that the optimum value for M is given by

$$M_{\mathrm{opt}} = \frac{p_d + w}{w}, \tag{3}$$

where p_d corresponds to the pixel size of the detector and w to the source size. The corresponding effective pixel size associated with M_{opt} is given by

$$p_{\mathrm{eff}} = \frac{w \cdot p_d}{w + p_d}. \tag{4}$$

Measuring beyond the limit using $M > M_{\mathrm{opt}}$, the geometric unsharpness leads to blurring and decreases the effective pixel size and thus the resolution. For our setup, where $w \approx 5$ μm and $p_d = 24$ μm, the optimal magnification factor amounts to $M_{\mathrm{opt}} \approx 5.8$ and the smallest achievable effective pixel size is $p_{\mathrm{eff,min}} \approx 4.14$ μm.

Another limitation at high magnification factors in DPC imaging is the decrease in sensitivity. The transverse shift of the interference fringes decreases proportionally to the source-to-sample distance and, therefore, inversely proportional to the magnification.[7]

In conclusion, we implemented a compact grating interferometer setup in a commercial SCANCO Medical μCT 100 system. A significant increase in FOV was achieved by developing flexible gratings which allow extremely short bending radii. A microfocus source provided enough spatial coherence for the interference formation as well as for high resolution imaging using geometric magnification. The minimal achievable effective pixel size allows resolutions comparable to synchrotron data.

The integration of grating interferometry in a micro CT scanner prototype opens the path for an immediate application of the multi-modal imaging technique in industrial devices.

We would like to thank Gordan Mikuljan for his support on the mechanical design, Simon Rutishauser for the fabrication of the planar gratings, and Stefan Haemmerle and Stephan Weiss from SCANCO Medical for the support on hardware and software interfacing in micro CT systems. This study was supported by Centre d'Imagerie BioMedicale (CIBM) of the UNIL, UNIGE, HUG, CHUV, EPFL and the Leenaards and Jeantet Foundations.

[1]C. David, B. Nöhammer, H. Solak, and E. Ziegler, Appl. Phys. Lett. **81**, 3287 (2002).
[2]A. Momose, Opt. Express **11**, 2303 (2003).
[3]T. Weitkamp, A. Diaz, C. David, F. Pfeiffer, M. Stampanoni, P. Cloetens, and E. Ziegler, Opt. Express **12**, 6296 (2005).
[4]F. Pfeiffer, M. Bech, O. Bunk, P. Kraft, E. Eikenberry, C. Brönnimann, C. Grünzweig, and C. David, Nature Mater. **7**, 134 (2008).
[5]A. Momose and J. Fukuda, Med. Phys. **22**, 375 (1995).
[6]F. Pfeiffer, T. Weitkamp, O. Bunk, and C. David, Nat. Phys. **2**, 258 (2006).
[7]M. Engelhardt, J. Baumann, M. Schuster, C. Kottler, F. Pfeiffer, O. Bunk, and C. David, Appl. Phys. Lett. **90**, 224101 (2007).
[8]C. David, J. Bruder, T. Rohbeck, C. Grünzweig, C. Kottler, A. Diaz, O. Bunk, and F. Pfeiffer, Microelectron. Eng. **84**, 1172 (2007).
[9]V. Revol, C. Kottler, R. Kaufmann, I. Jerjen, T. Lüthi, F. Cardot, P. Niedermann, U. Straumann, U. Sennhauser, and C. Urban, Nucl. Instrum. Methods Phys. Res. Sec. A (in press).
[10]J. Kenntner, T. Grund, B. Matthis, M. Boerner, J. Mohr, T. Scherer, M. Walter, M. Willner, A. Tapfer, M. Bech, F. Pfeiffer, I. Zanette, and T. Weitkamp, Proc. SPIE **7804**, 780408 (2010).
[11]B. Blakeley and K. Spartiotis, Insight Nondestr. Test. Cond. Monit. **48**, 109 (2006).